

PHY 564

Advanced Accelerator Physics

Lecture 26

Nonlinear elements and nonlinear dynamics. Part II

Vladimir N. Litvinenko
Yichao Jing
Gang Wang

CENTER for ACCELERATOR SCIENCE AND EDUCATION
Department of Physics & Astronomy, Stony Brook University
Collider-Accelerator Department, Brookhaven National Laboratory

Third order Resonances

$$H = \frac{1}{2} x'^2 + \frac{1}{2} K_x(s) x^2 + \frac{1}{2} z'^2 + \frac{1}{2} K_z(s) z^2 - e A_{s,NL}(x, z, s)$$

$$\tilde{H} = \nu_x J_x + \nu_z J_z - e A_{s,NL}(J_x, \psi_x, J_z, \psi_z, \theta)$$

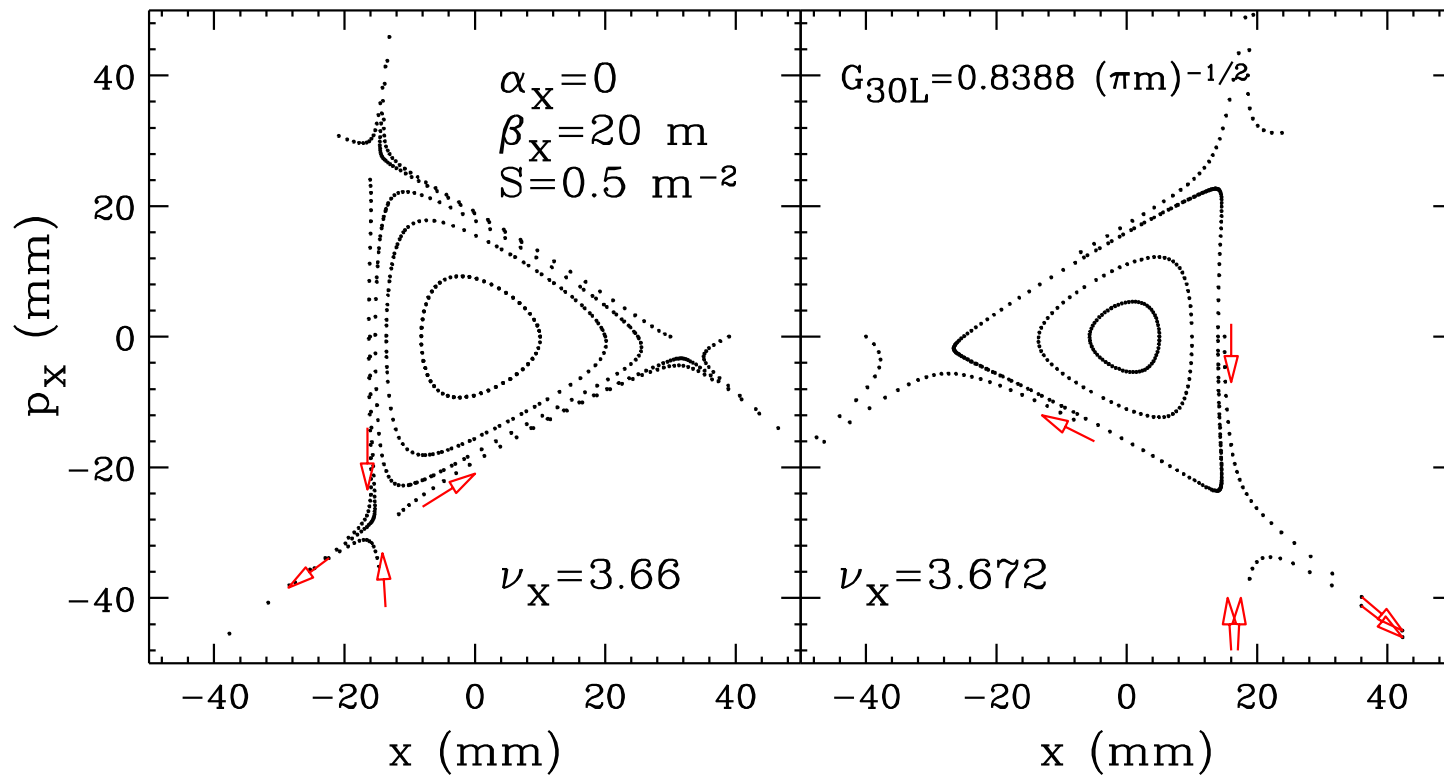
$$A_x = A_z = 0, \quad A_s = \frac{B_2}{6}(x^3 - 3xz^2), \quad B_2 = \partial^2 B_z / \partial x^2 \big|_{x=z=0}$$

$$H = \frac{1}{2} [x'^2 + K_x x^2 + z'^2 + K_z z^2] + V_3(x, z, s),$$

$$V_3(x, z, s) = \frac{1}{6} S(s) (x^3 - 3xz^2) \qquad S(s) = -\frac{B_2(s)}{B\rho}$$

$$x'' + K_x(s)x = -\frac{1}{2}S(s)(x^2 - z^2), \quad z'' + K_z(s)z = +S(s)xz.$$

$$\Delta x' = -\frac{1}{2}\bar{S}(x^2 - z^2), \quad \Delta z' = \bar{S}xz.$$



The Poincaré maps for betatron motion perturbed by a single sextupole magnet at a tune below (left) and above (right) a third order resonance. The integrated sextupole strength is $S=0.5\text{m}^{-2}$ with lattice parameters $\beta_x=20\text{m}$, and $\alpha_x=0$. Arrows indicate directions of motion near a separatrix.

The leading order resonances driven by sextupoles

$$y = \sqrt{2\beta\bar{J}} \cos(\bar{\psi} + \chi(s) - \nu\theta),$$

$$\mathcal{P}_y = \beta y' + \alpha y = -\sqrt{2\beta\bar{J}} \sin(\bar{\psi} + \chi(s) - \nu\theta),$$

$$\chi(s) = \int_0^s \frac{ds}{\beta}$$

$$x = \sqrt{2\beta_x J_x} \cos \Phi_x, \quad z = \sqrt{2\beta_z J_z} \cos \Phi_z$$

$$\Phi_x = \psi_x + \chi_x(s) - \nu_x \theta, \quad \Phi_z = \psi_z + \chi_z(s) - \nu_z \theta$$

$$H = \frac{1}{2} [x'^2 + K_x x^2 + z'^2 + K_z z^2] + V_3(x, z, s),$$

$$V_3(x, z, s) = \frac{1}{6} S(s) (x^3 - 3xz^2)$$

$$\begin{aligned} V_3 &= \frac{1}{6} S(s) [2^{3/2} \beta_x^{3/2} J_x^{3/2} \cos^3 \Phi_x - 3 \cdot 2^{3/2} \beta_x^{1/2} J_x^{1/2} \beta_z J_z \cos \Phi_x \cos^2 \Phi_z] \\ &= \frac{\sqrt{2}}{12} S(s) \beta_x^{3/2} J_x^{3/2} \cos 3(\psi_x + \chi(s) - \nu_x \theta) + \dots \end{aligned}$$

$$H = \nu_x J_x + \nu_z J_z + \sum_{\ell} G_{3,0,\ell} J_x^{3/2} \cos(3\psi_x - \ell\theta + \xi_{3,0,\ell}) + \dots$$

$$G_{3,0,\ell} e^{j\xi_{3,0,\ell}} = \frac{\sqrt{2}}{24\pi} \oint S(s) \beta_x^{3/2} \exp(j[3\chi(s) - (3\nu_x - \ell)\theta]) ds$$

$$\begin{aligned}
H = & \nu_x J_x + \nu_z J_z + \sum_{\ell} G_{3,0,\ell} J_x^{3/2} \cos(3\phi_x - \ell\theta + \xi_{3,0,\ell}) \\
& + \sum_{\ell} G_{1,2,\ell} J_x^{1/2} J_z \cos(\phi_x + 2\phi_z - \ell\theta + \xi_{1,2,\ell}) \\
& + \sum_{\ell} G_{1,-2,\ell} J_x^{1/2} J_z \cos(\phi_x - 2\phi_z - \ell\theta + \xi_{1,-2,\ell}) + \cdots,
\end{aligned}$$

where ℓ is an integer, $G_{3,0,\ell}$, $G_{1,2,\ell}$, $G_{1,-2,\ell}$ are Fourier amplitudes, $\xi_{3,0,\ell}$, $\xi_{1,2,\ell}$, $\xi_{1,-2,\ell}$ are the phase of the Fourier components, and \cdots describes the remaining resonance driving terms at $\nu_x = \text{integers}$. The Fourier amplitude $G_{3,0,\ell}$ drives the third order resonance at $3\nu_x = \ell$, and similarly, $G_{1,2,\ell}$ and $G_{1,-2,\ell}$ drive $\nu_x + 2\nu_z = \ell$ and $\nu_x - 2\nu_z = \ell$ resonances.

The third order resonance at $3\nu_x = \ell$

The Hamiltonian near a third-order resonance at $3\nu_x = \ell$ is

$$H \approx \nu_x J_x + G_{3,0,\ell} J_x^{3/2} \cos(3\phi_x - \ell\theta + \xi)$$

where $G_{3,0,\ell}$ is the resonance strength, J_x, ϕ_x are conjugate phase-space coordinates, θ is the orbiting angle serving time coordinate, ν_x is the horizontal betatron tune.

$$G_{3,0,\ell} e^{j\xi_{3,0,\ell}} = \frac{\sqrt{2}}{24\pi} \oint \beta_x^{3/2} K_2(s) e^{j[3\chi_x(s) - (3\nu_x - \ell)\theta]} ds$$

Transform the phase space coordinate to a *resonance rotating frame* with a generating function to obtain new phase-space coordinates:

$$F_2 = \left(\phi_x - \frac{\ell}{3}\theta + \frac{\xi}{3}\right)J, \quad \Rightarrow \quad \phi = \phi_x - \frac{\ell}{3}\theta + \frac{\xi}{3}, \quad J = J_x.$$

The new Hamiltonian and Hamilton's equations of motion are

$$H = \delta J + G_{3,0,\ell} J^{3/2} \cos 3\phi,$$
$$\dot{\phi} \equiv \frac{d\phi}{d\theta} = \delta + \frac{3}{2}G_{3,0,\ell} J^{1/2} \cos 3\phi, \quad \dot{J} \equiv \frac{dJ}{d\theta} = 3G_{3,0,\ell} J^{3/2} \sin 3\phi.$$

where $\delta = \nu_x - \ell/3$ is the resonance proximity parameter.

The fixed points (FPs) of the Hamiltonian are determined by $dJ/d\theta=0$ and $d\phi/d\theta=0$. Without nonlinear detuning, there is no stable fixed point for the third order resonance. The action and Hamiltonian value at the UFP, and small amplitude motion near the UFP are

$$J_{\text{UFP}}^{1/2} = \left| \frac{2\delta}{3G_{3,0,\ell}} \right| \quad \text{with} \quad \begin{cases} \phi_{\text{FP}} = 0, \pm 2\pi/3, & \text{if } \delta/G_{3,0,\ell} < 0, \\ \phi_{\text{FP}} = \pm\pi/3, \pi, & \text{if } \delta/G_{3,0,\ell} > 0. \end{cases}$$

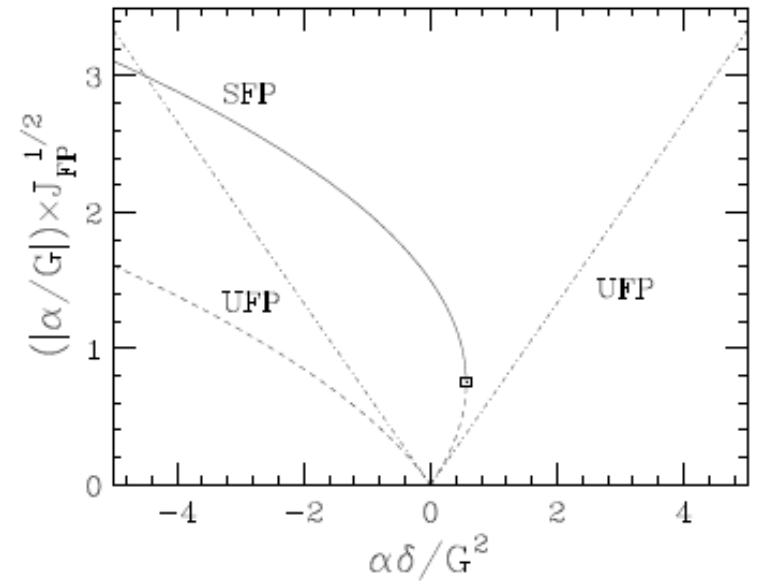
$$E_{\text{UFP}} = \frac{\delta}{3} \left(\frac{2\delta}{3G_{3,0,\ell}} \right)^2,$$

$$\ddot{K} - 3\delta^2 K - 6 \frac{\delta^2}{J_{\text{UFP}}} K^2 = 0, \quad K = J - J_{\text{UFP}}$$

The motion near the fixed point is hyperbolic. Because of nonlinear term in the Equation above, the amplitude will grow faster than an exponential. The direction of particle motion near a separatrix is marked with arrows in the Figure.

Without a nonlinear detuning term, the third-order resonance appears at all values of δ . The stable motion is bounded by the curve of $J_{\text{UFP}}^{1/2}$. For a given aperture J_{max} the width of the third-order betatron resonance is

$$|\delta|_{\text{width}} = 3G_{3,0,\ell} \hat{J}^{1/2} / 2.$$



Separatrix

The separatrix is the Hamiltonian torus that passes through the UFP, i.e. $H = E_{\text{UFP}}$. The separatrix orbit, for $\delta/G_{3,0,\ell} > 0$,

$$[2X - 1] \left[P - \frac{1}{\sqrt{3}}(X + 1) \right] \left[P + \frac{1}{\sqrt{3}}(X + 1) \right] = 0$$

$$X = \sqrt{J/J_{\text{UFP}}} \cos \phi, \quad P = -\sqrt{J/J_{\text{UFP}}} \sin \phi$$

$$X = 1/2$$

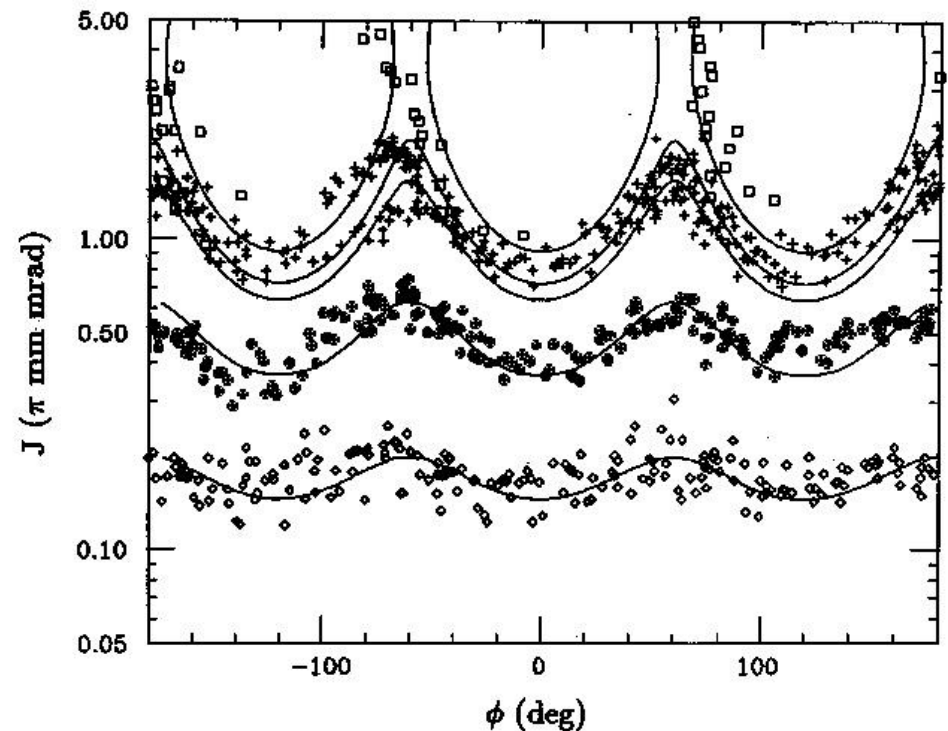
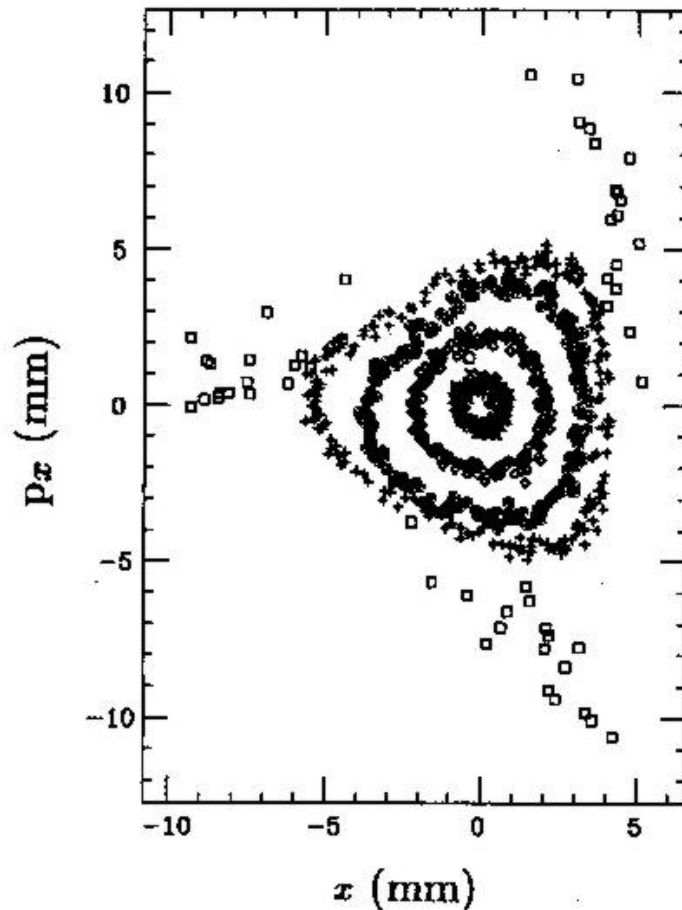
$$P = \frac{1}{\sqrt{3}}(X + 1)$$

$$P = -\frac{1}{\sqrt{3}}(X + 1)$$

$$(X, P)_{\text{UFP}} = (-1, 0), \quad \left(\frac{1}{2}, \frac{\sqrt{3}}{2}\right), \quad \left(\frac{1}{2}, -\frac{\sqrt{3}}{2}\right)$$

Nonlinearity in accelerators has been employed to provide

- Beam manipulations such as slow extraction, beam dilution
- Landau damping for collective beam instabilities
- Overcoming spin depolarization resonances



Nonlinear detuning parameters:

Accelerator magnets may have many nonlinear magnetic multipoles. Some of them can introduce nonlinear perturbation to betatron motion, e.g.

$$V(s) = \frac{1}{6}K_2(s)(x^3 - 3xz^2) + \frac{1}{24}K_3(s)(x^4 - 6x^2z^2 + z^4) + \dots$$

With Floquet transformation, the Hamiltonian becomes

$$H = \nu_x J_x + \nu_z J_z + \frac{1}{2} \alpha_{xx} J_x^2 + \alpha_{xz} J_x J_z + \frac{1}{2} \alpha_{zz} J_z^2 + \dots$$

$$\alpha_{xx} = \frac{1}{16\pi} \oint \beta_x^2 K_3 ds, \quad \alpha_{xz} = \frac{-1}{8\pi} \oint \beta_x \beta_z K_3 ds, \quad \alpha_{zz} = \frac{1}{16\pi} \oint \beta_z^2 K_3 ds.$$

$$Q_x = \frac{d\psi_x}{d\theta} = \frac{\partial H}{\partial J_x} \approx \nu_x + \alpha_{xx} J_x + \alpha_{xz} J_z + \dots$$

$$Q_z = \frac{d\psi_z}{d\theta} = \frac{\partial H}{\partial J_z} \approx \nu_z + \alpha_{xz} J_x + \alpha_{zz} J_z + \dots$$

The coefficients α 's are called nonlinear detuning parameters

Betatron detuning: chromaticity $\Delta\nu_y = C_y^{(1)}\delta + C_y^{(2)}\delta^2 + \dots$

octupole
$$\begin{aligned} Q_x &= \nu_x + \alpha_{xx}J_x + \alpha_{xz}J_z \\ Q_z &= \nu_z + \alpha_{xz}J_x + \alpha_{zz}J_z. \end{aligned} + \dots$$

$$\alpha_{xx} = \frac{1}{16\pi} \oint \beta_x^2 K_3 ds, \quad \alpha_{xz} = \frac{-1}{8\pi} \oint \beta_x \beta_z K_3 ds, \quad \alpha_{zz} = \frac{1}{16\pi} \oint \beta_z^2 K_3 ds.$$

sextupole

$$\begin{aligned} \alpha_{xx} &= \frac{1}{64\pi} \sum_{i,j} S_i S_j \beta_{x,i}^{3/2} \beta_{x,j}^{3/2} \left[\frac{\cos 3(\pi\nu_x - |\psi_{x,ij}|)}{\sin 3\pi\nu_x} + 3 \frac{\cos(\pi\nu_x - |\psi_{x,ij}|)}{\sin \pi\nu_x} \right], \\ \alpha_{xz} &= \frac{1}{32\pi} \left\{ \sum_{i,j} S_i S_j \beta_{x,i}^{1/2} \beta_{x,j}^{1/2} \beta_{z,i} \beta_{z,j} \left[\frac{\cos[2(\pi\nu_z - |\psi_{z,ij}|) + \pi\nu_x - |\psi_{x,ij}|]}{\sin \pi(2\nu_z + \nu_x)} \right. \right. \\ &\quad \left. \left. + \frac{\cos[2(\pi\nu_z - |\psi_{z,ij}|) - (\pi\nu_x - |\psi_{x,ij}|)]}{\sin \pi(2\nu_z - \nu_x)} \right] \right. \\ &\quad \left. - 2 \sum_{i,j} S_i S_j \beta_{x,i}^{3/2} \beta_{x,j}^{1/2} \beta_{z,j} \frac{\cos(\pi\nu_x - |\psi_{x,ij}|)}{\sin \pi\nu_x} \right\}, \\ \alpha_{zz} &= \frac{1}{64\pi} \sum_{i,j} S_i S_j \beta_{x,i}^{1/2} \beta_{x,j}^{1/2} \beta_{z,i} \beta_{z,j} \left[\frac{\cos[2(\pi\nu_z - |\psi_{z,ij}|) + \pi\nu_x - |\psi_{x,ij}|]}{\sin \pi(2\nu_z + \nu_x)} \right. \\ &\quad \left. + \frac{\cos[2(\pi\nu_z - |\psi_{z,ij}|) - (\pi\nu_x - |\psi_{x,ij}|)]}{\sin \pi(2\nu_z - \nu_x)} + 3 \frac{\cos(\pi\nu_x - |\psi_{x,i} - \psi_{x,j}|)}{\sin \pi\nu_x} \right], \end{aligned}$$

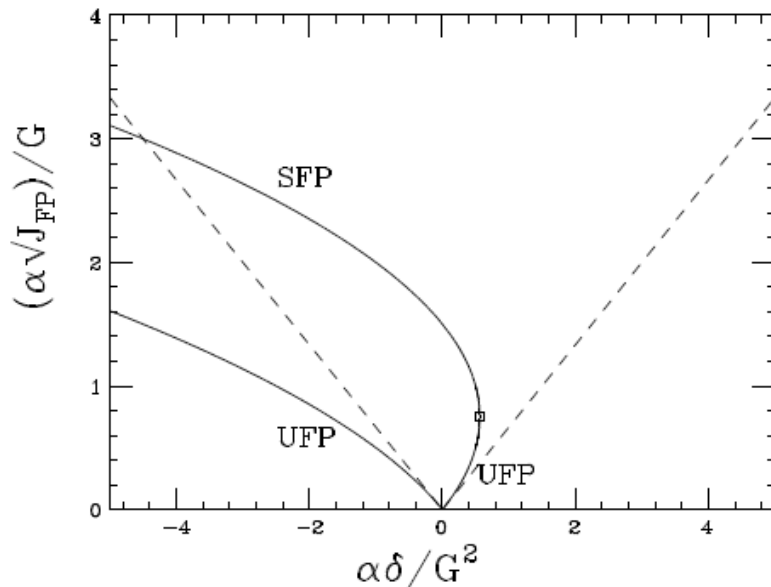
Effect of nonlinear detuning

Nonlinear magnetic multipoles also generate nonlinear betatron detuning, i.e. the betatron tunes depend on the betatron actions. Including the effect of nonlinear betatron detuning, the Hamiltonian near a third-order resonance is

$$H = \delta J + \frac{1}{2}\alpha J^2 + GJ^{3/2} \cos 3\phi$$

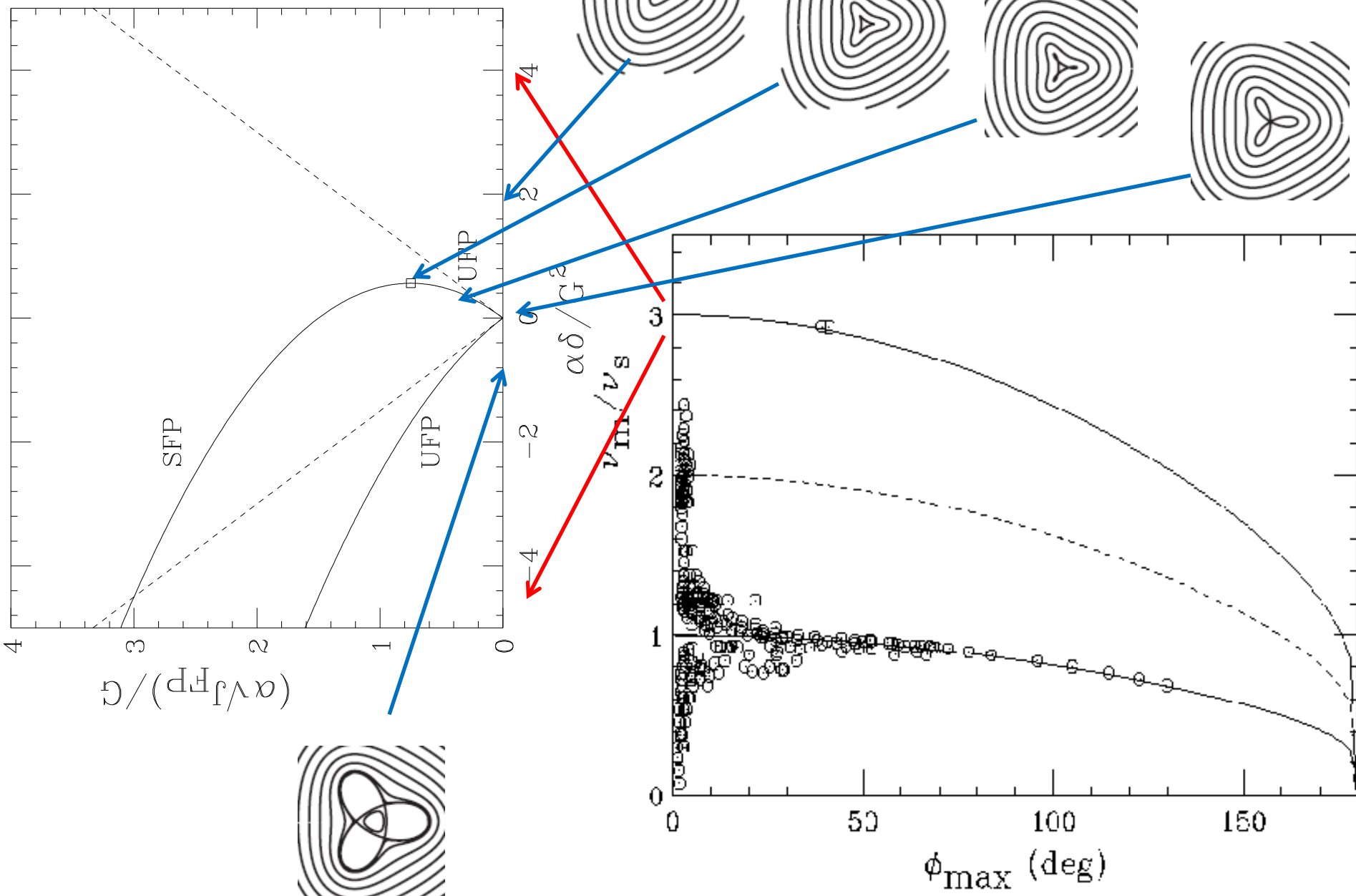
With nonlinear detuning, stable fixed points appear. The fixed points of the Hamiltonian for $\alpha > 0$ and $G > 0$ are

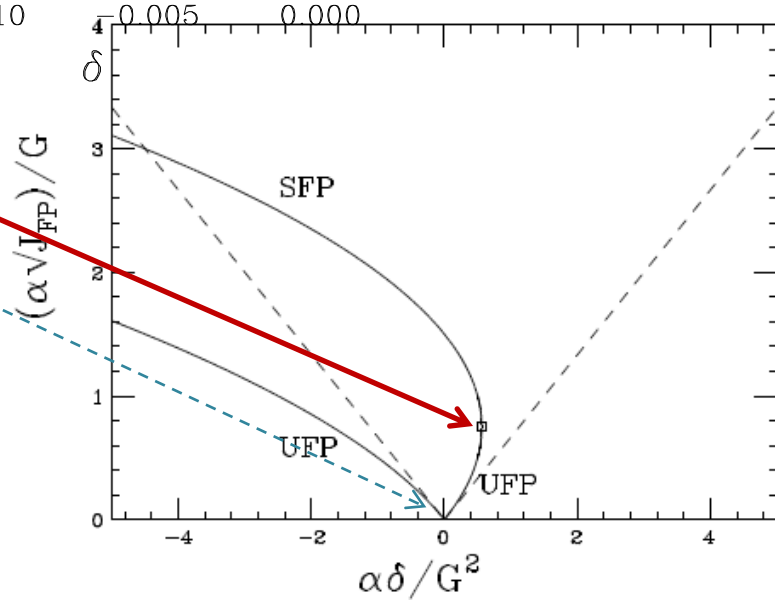
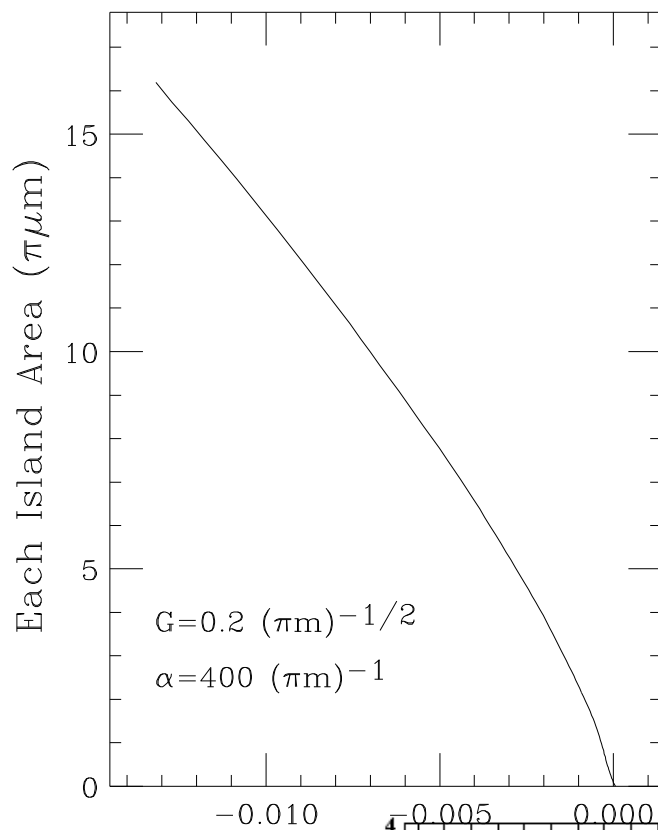
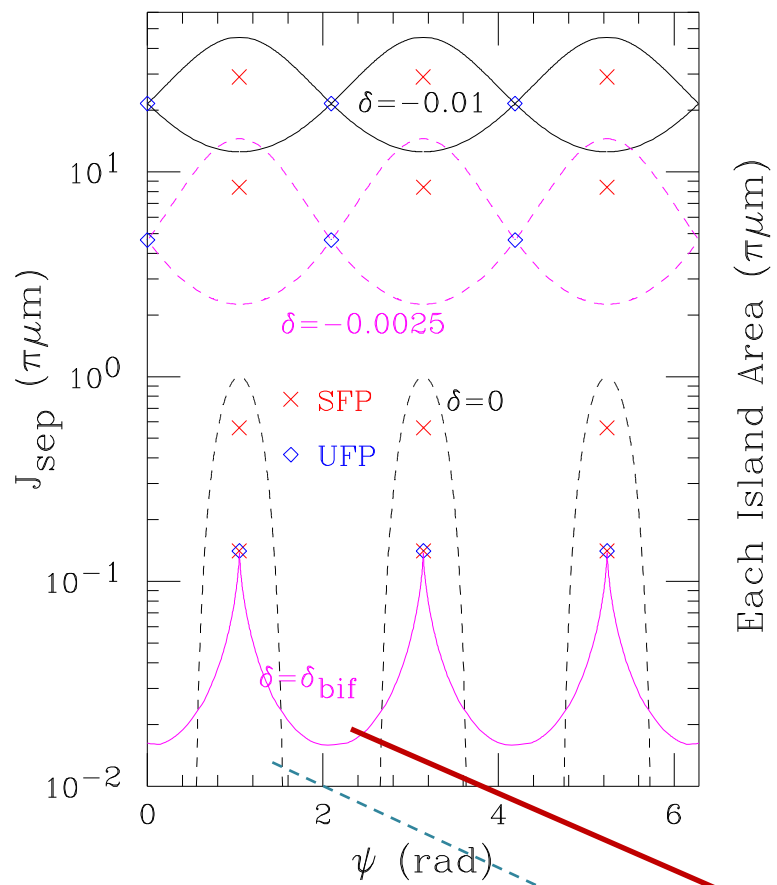
$$\frac{\alpha J_{\text{FP}}^{1/2}}{G} = \begin{cases} -\frac{3}{4} + \frac{3}{4} \sqrt{1 - \frac{16\alpha\delta}{9G^2}}, & \phi = 0, \pm 2\pi/3 \quad \delta < 0 \quad (\text{UFP}) \\ +\frac{3}{4} - \frac{3}{4} \sqrt{1 - \frac{16\alpha\delta}{9G^2}}, & \phi = \pi, \pm \pi/3 \quad 0 \leq \delta \leq \frac{9G_{3,0,\ell}^2}{16\alpha} \quad (\text{UFP}) \\ +\frac{3}{4} + \frac{3}{4} \sqrt{1 - \frac{16\alpha\delta}{9G^2}}, & \phi = \pi, \pm \pi/3 \quad \delta \leq \frac{9G^2}{16\alpha} \quad (\text{SFP}) \end{cases}$$



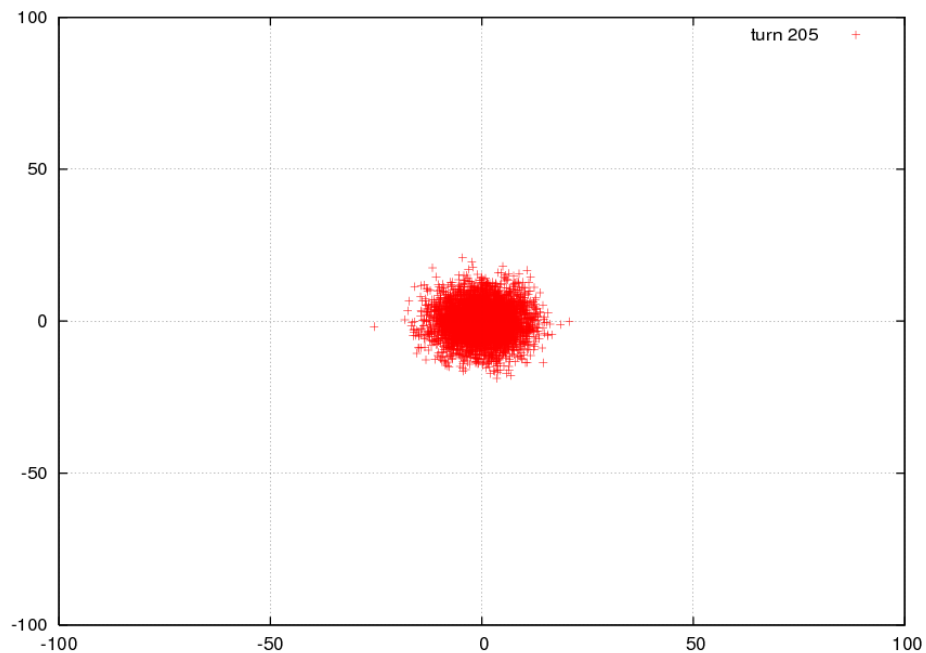
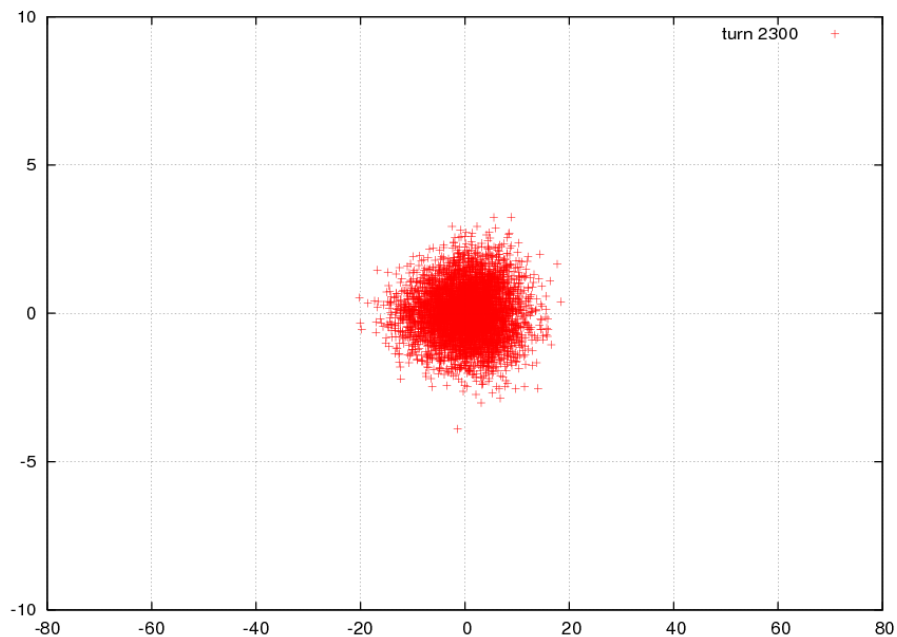
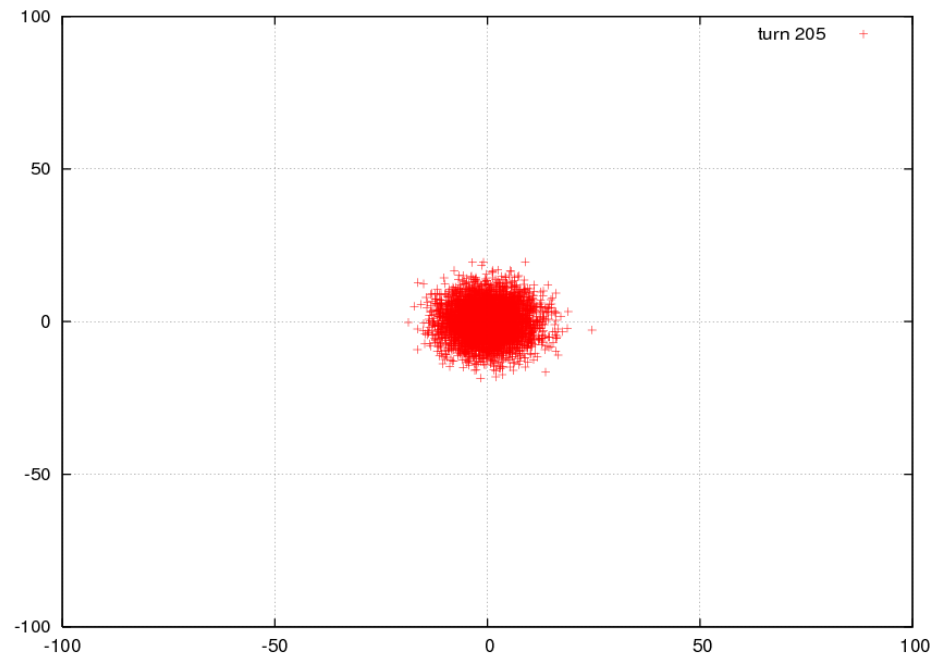
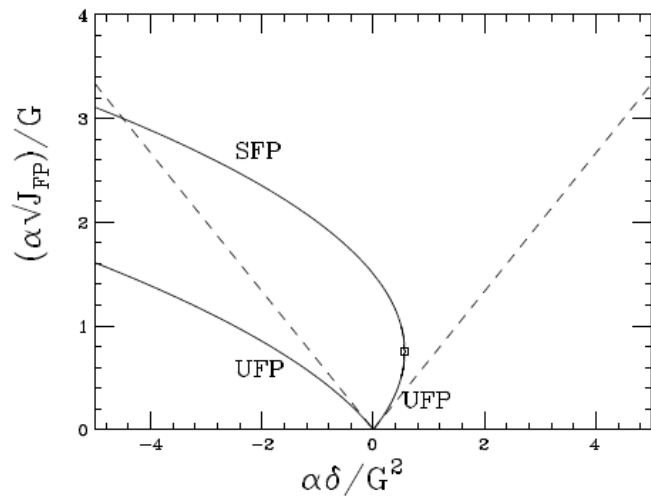
The bifurcation of third-order resonance islands occurs at $16\alpha\delta \leq 9G_{3,0,\ell}^2$. The Figure shows $\alpha J_{\text{UFP}}^{1/2}/|G_{3,0,\ell}|$ vs $\alpha\delta/G_{3,0,\ell}^2$ for the bifurcation of third-order resonance.

Sextupole 3rd resonance

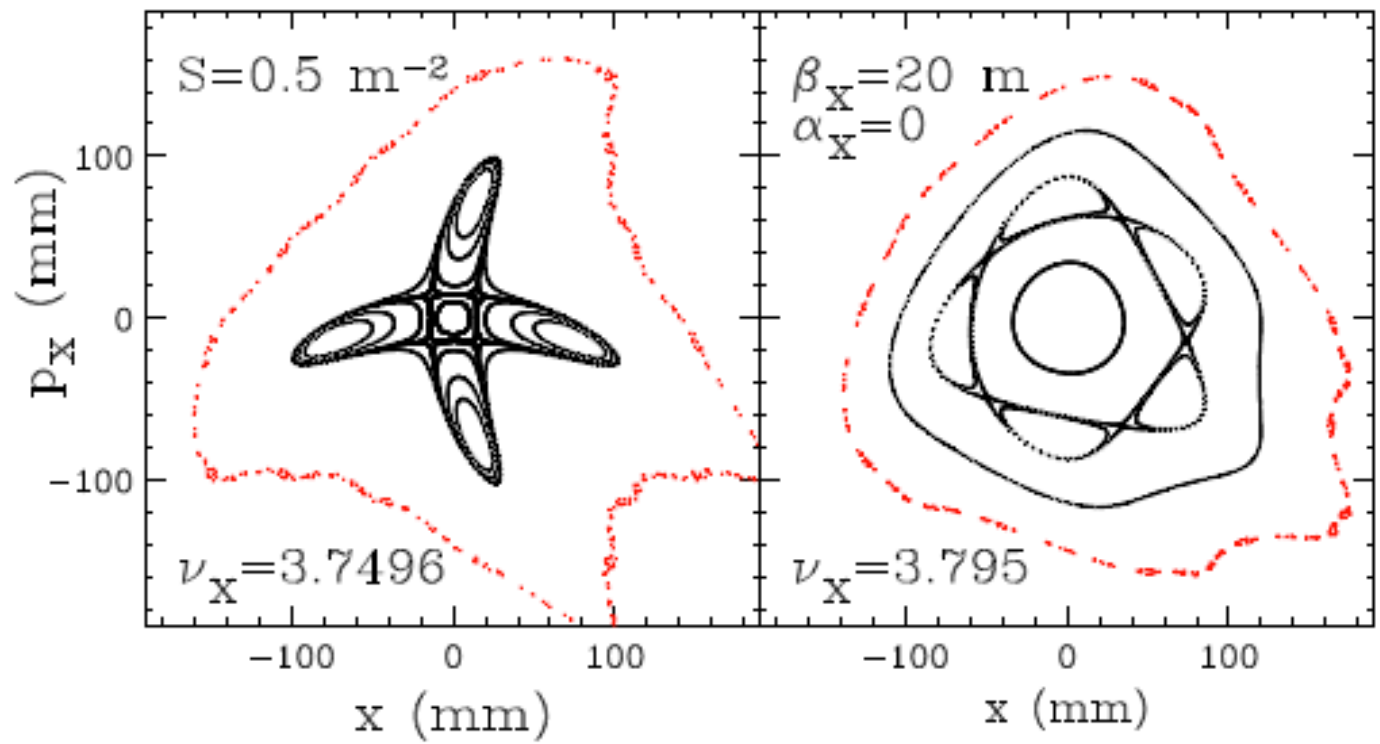




Nonlinear beam dynamics on resonance crossing



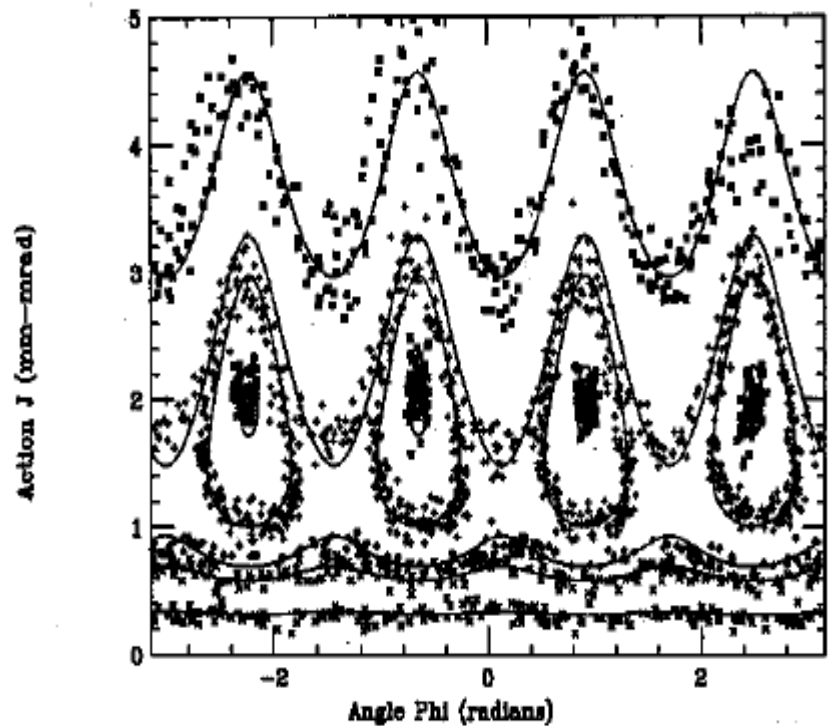
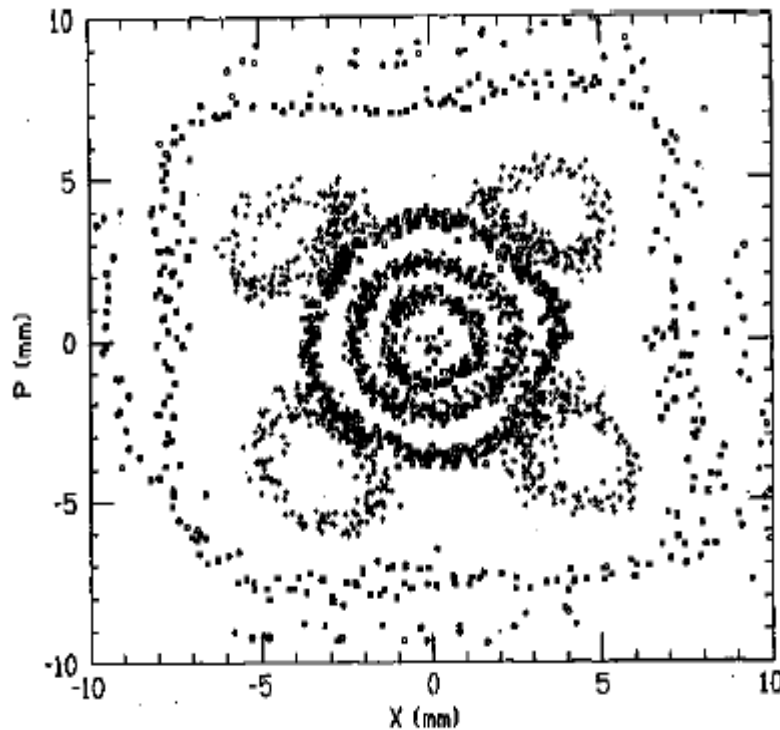
It appears that sextupoles will not produce resonances higher than the third order ones listed earlier. However, strong sextupoles are usually needed to correct chromatic aberration. Concatenation of strong sextupoles can generate high-order resonances such as $4\nu_x$, $2\nu_x \pm 2\nu_z$, $4\nu_z$, $5\nu_x$, \dots , etc. The Figure below shows the Poincaré maps of the single sextupole model at $\nu_x=3.7496$ and $\nu_x=3.795$, i.e. a single sextupole can also drive the fourth and higher order resonances. One can use a canonical perturbation method to explain the tracking result. Since resonance islands only exist with $\nu_x < 3.75$ or $\nu_x < 3.8$, the effective nonlinear detuning must be positive. The largest phase space map marks the boundary of stable motion.



Near a *weak* fourth-order 1D resonance, the Hamiltonian can normally be approximated by

$$H = \nu_x J_x + \frac{1}{2} \alpha_{xx} J_x^2 + G_{4,0,\ell} J_x^2 \cos(4\psi_x - \ell\theta + \xi_{4,0,\ell}),$$

$$G_{4,0,\ell} e^{j\xi_{4,0,\ell}} = \frac{1}{96\pi} \oint \beta_x^2 K_3(s) e^{j[4\chi_x(s) - (4\nu_x - \ell)\theta]} ds,$$

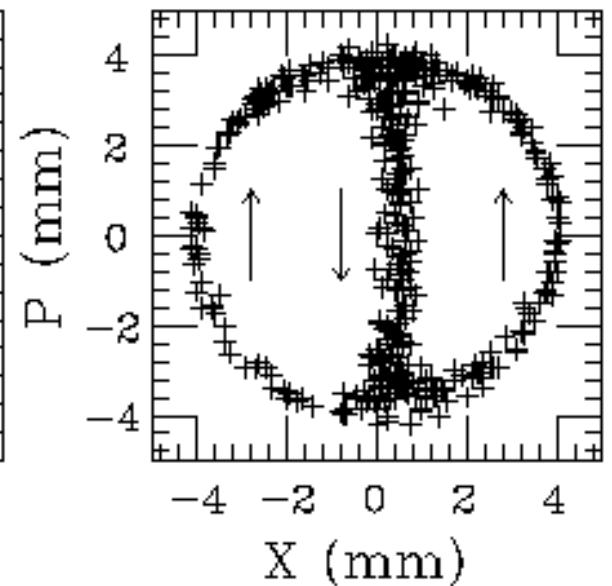
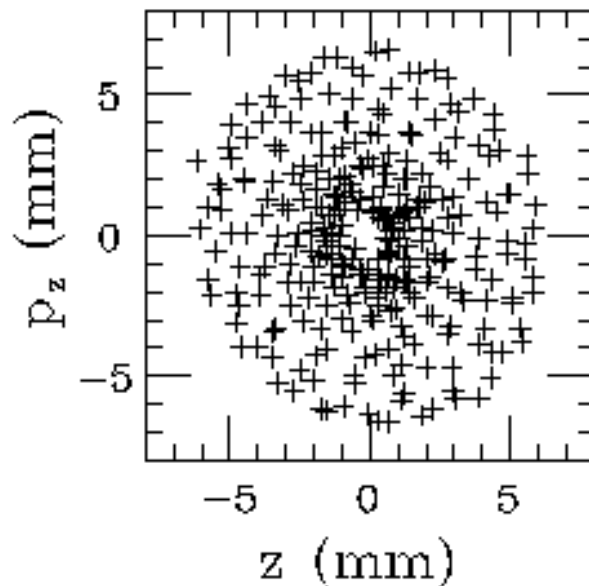
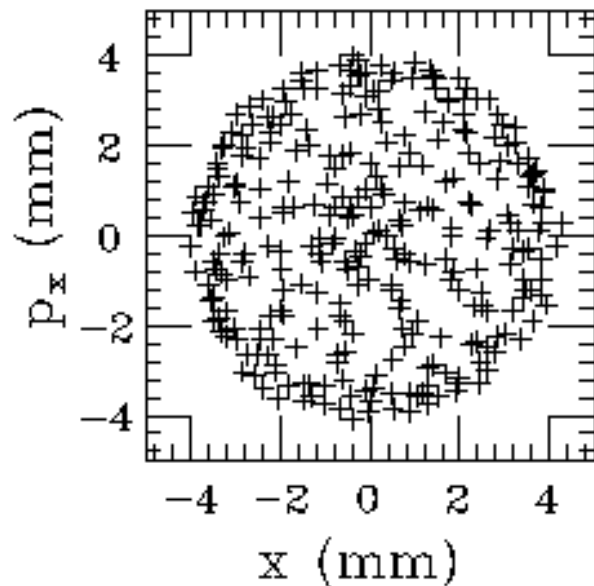
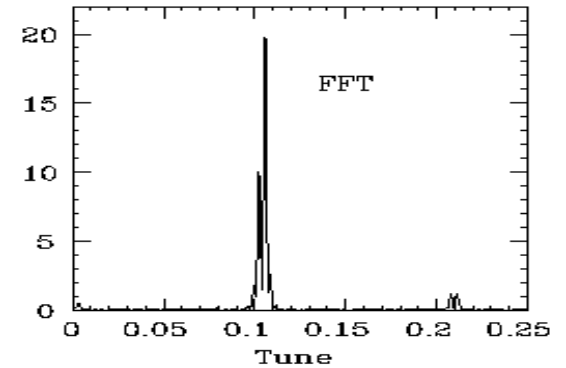
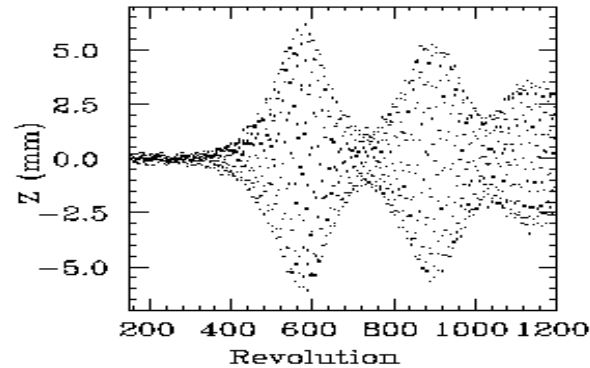
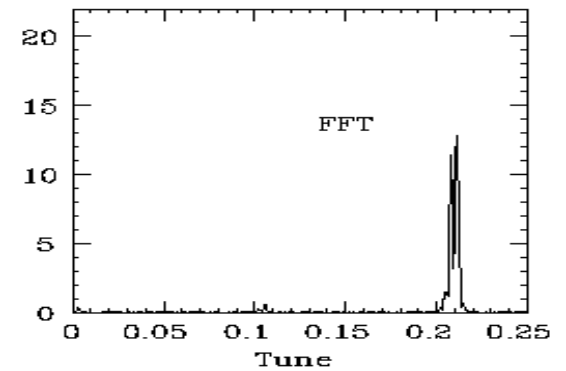
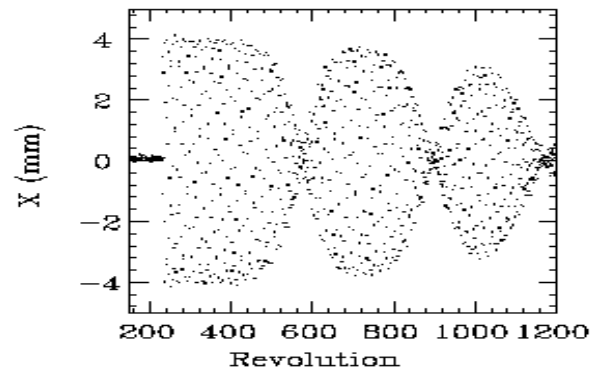


The solid lines are the Hamiltonian tori with parameters $\alpha_{xx}=650(\pi\text{m})^{-1}$, $G_{4,0,15}=80(\pi\text{m})^{-1}$, and $\nu_x-3.75=-7.8\times 10^{-4}$.

$$v_x - 2 v_z = \ell$$

The betatron phase space can be visualized as a space filled by invariant tori, even near a nonlinear resonance.

For a difference resonance, the invariant is bounded!



- The studies of **sum resonances** are not as successful. We have constructed a tune jump quadrupole to move betatron tunes onto a sum resonance $\nu_x + 2\nu_z$ and observed betatron amplitude growth obeying the invariant at the resonance.
- Take $2\nu_x + 2\nu_z$ resonance as an example, we expect to see particle loss through tori as shown in the graph below. This means that the betatron phase space is filled with resonance lines, where particles that locked onto a resonance will leak out to a large amplitude betatron motion through these resonance tori. The invariant tori are unbounded for sum resonances!
- **Experiments has yet to be carried out!**

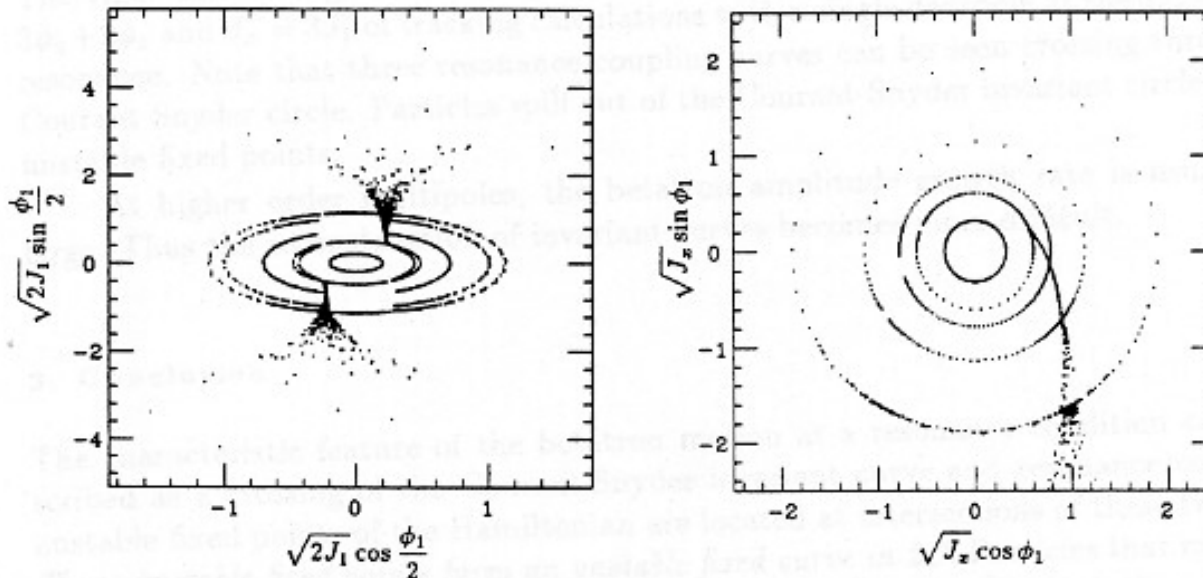
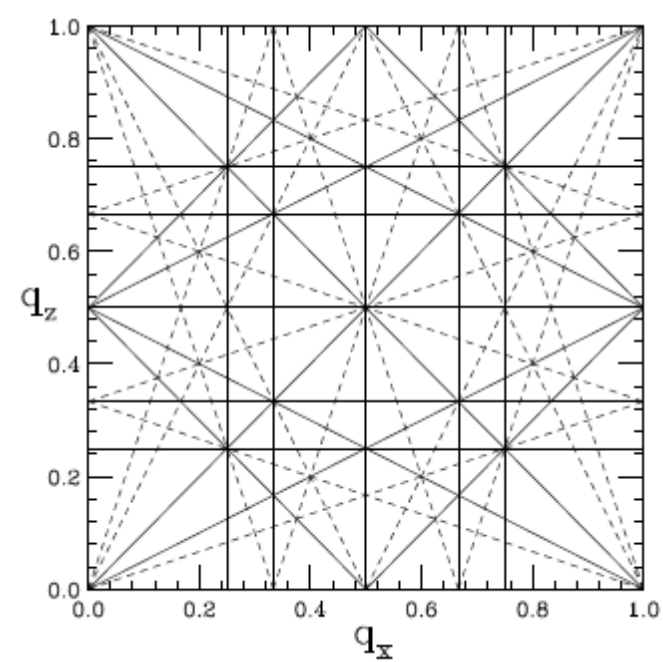
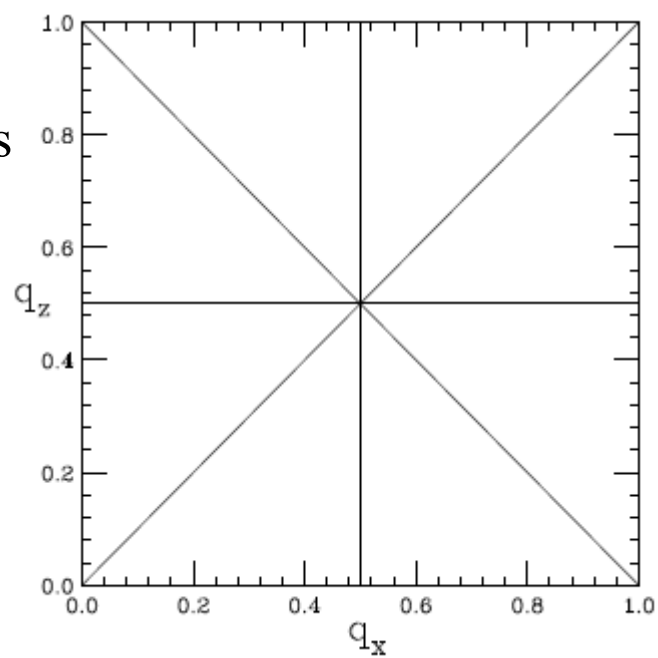
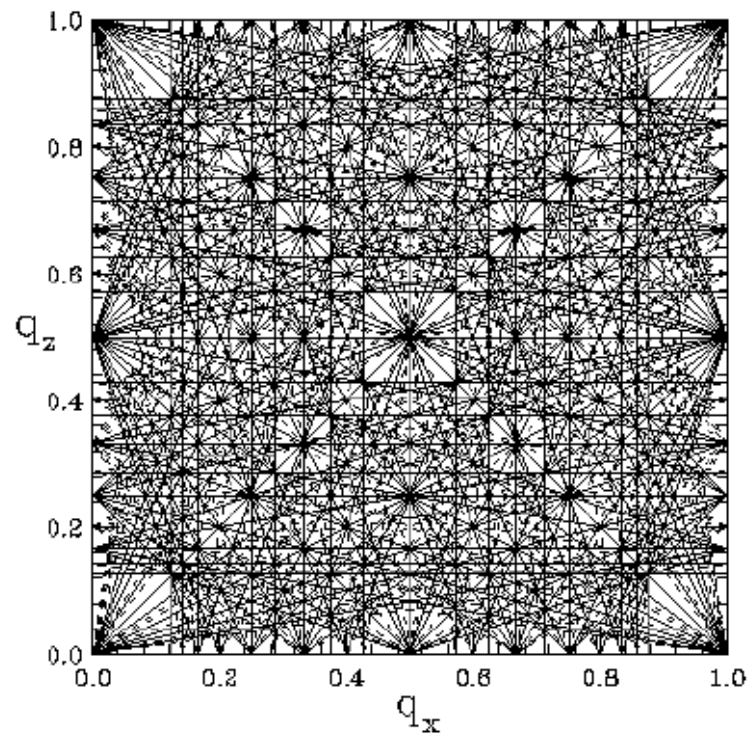


Figure 3. The Poincaré maps (see text for explanation) are shown for a Simple tracking calculation with a single octupole at a $2\nu_x + 2\nu_z = \ell$ resonance.

Linear resonances

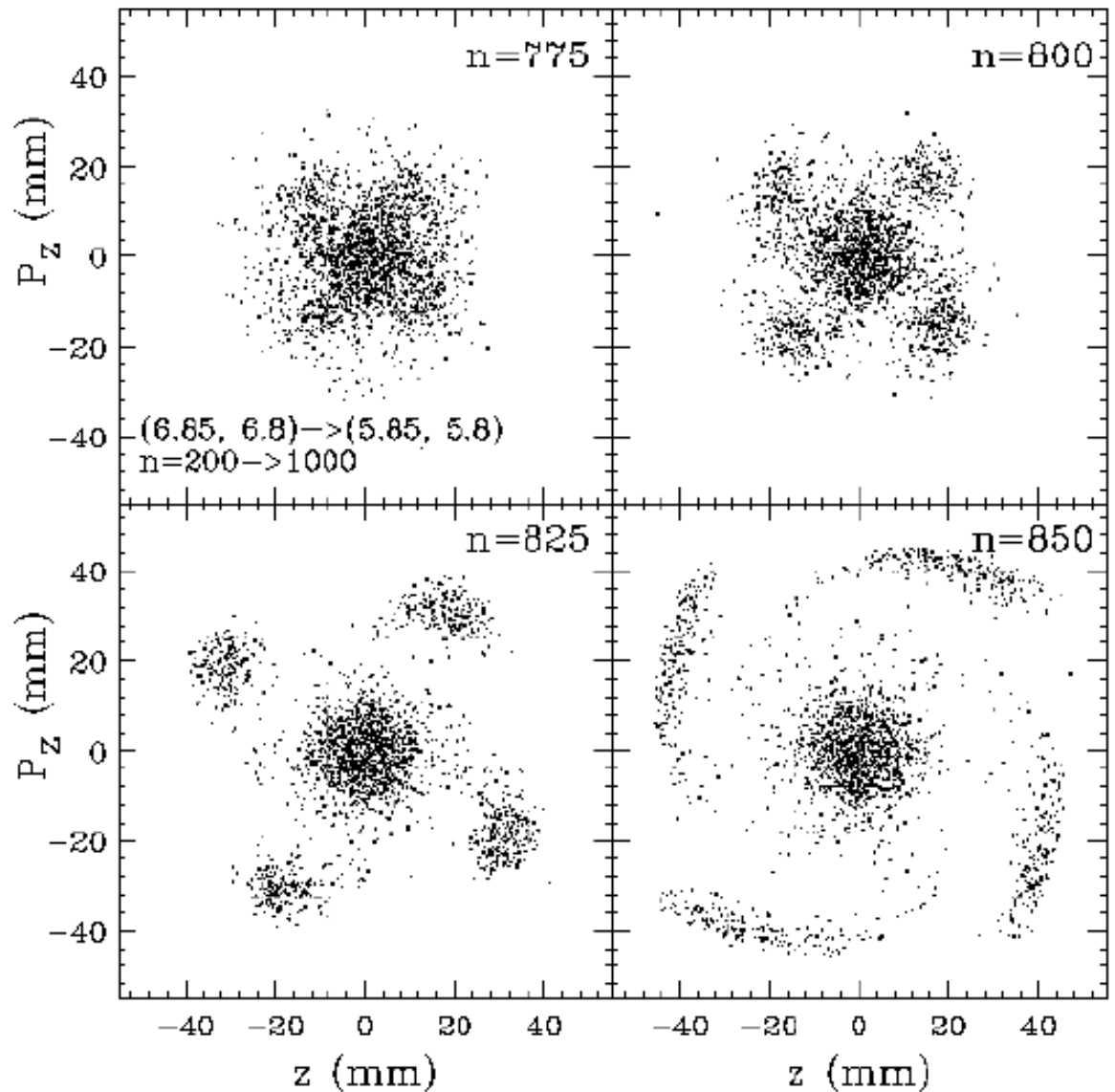


Resonances up to 4th order



Up to 8th order resonances

Space charge resonances in high power accelerators



The next effect, which is important, is stochastic trajectories, which appear in the motion of the particles (turn by turn) – see Fig. 11. One of a simple criteria which was developed is called Chirikov criteria, stating that that stochastic layer in Poincare diagrams (the particles motion) appears when two non-linear resonances overlap. Careful look into fig 11 reveals that in addition to main resonance (4th and 3rd order) there are additional high order resonance (islands) formed – some of them clearly identifiable, some destroyed and turned into a stochastic layer. Usually stochastic layer cause loss of particles at large amplitudes. It is also typical (with exception of beam-beam effects, when the nonlinearity of the beam is of the order of the beam size) that motion at large amplitudes becomes unstable and chaotic. Area of the dynamically (not physically) stable motion of particles is called “dynamic aperture” or DA.

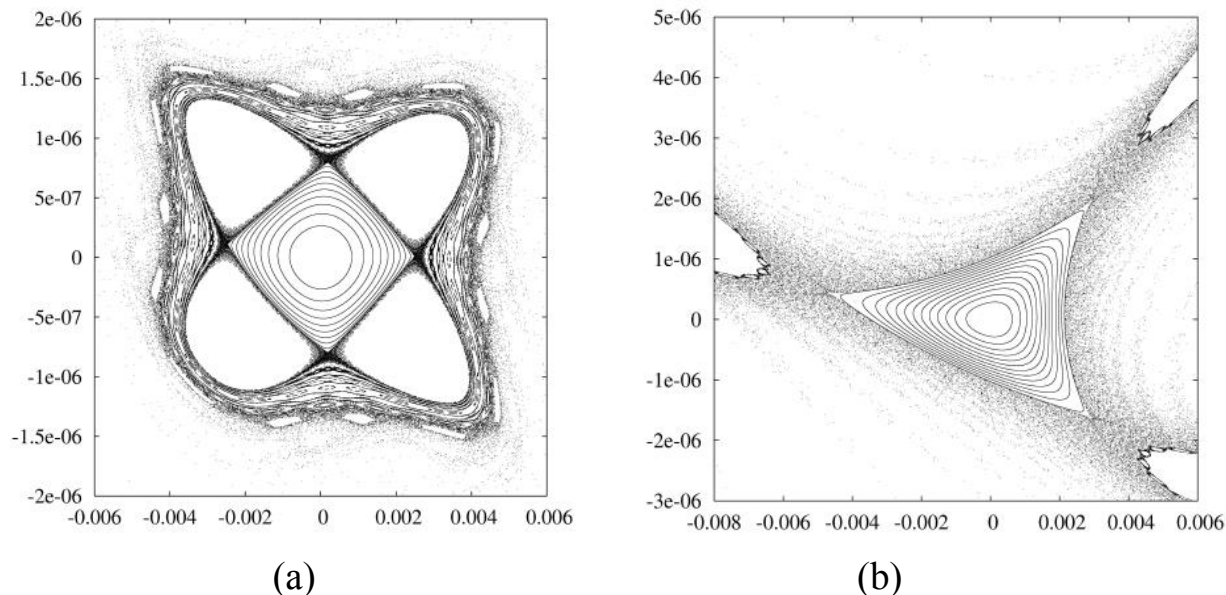


Fig.11. Two tracking results: (a) with 4th order and (b) 3rd order resonance strictures.

Methods of increasing dynamic aperture are multiple and there is no one specific trick (or set of tricks), which does the magic – to a degree it remains to be an art form. Still, reducing strength of the resonant terms and low order geometrical distortion are necessary steps in creating modern accelerator with large dynamic aperture.

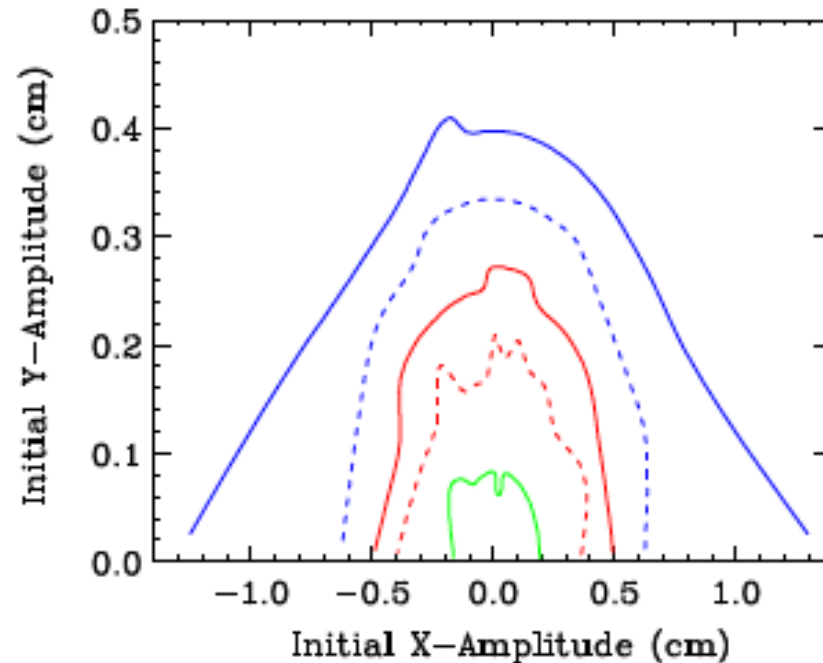


Fig.12. Momentum dependent dynamic aperture for 4th-order geometrical achromat (with zero chromaticity) Energy offsets: 0% - blue solid, 0.5% - dashed blue, 1% - red solid, 1.5% - dashed red, 1.5% - green. The dynamic aperture shown in a specific place in the storage ring – particles launched outside the dynamic aperture do not survive and are lost at large amplitudes.

Computers playing important role in both generating and analyzing non-linear maps. There is a very strong link to cosmology, which faces problems similar to that in modern accelerators - a long-time tracking of solar and star systems. One the modern tools in DA studies is borrowed from cosmology and called frequency map analysis (FMA) – the idea is to characterize how chaotic is the motion of particles with given amplitude of oscillations.

If we perform a discrete Fourier transform on the tracking data (starting with an initial x-y) position and obtain the betatron tunes (for N turn tracking, the precision is 1/N). If we repeat this process with different initial positions, we can obtain a tune map. To indicate the variation of the tunes over different turns of the ring, we can define a diffusion or regularity, which describes the difference between the tunes over various periods (usually the first half of the tracking (Q_{x1} , Q_{y1}) and the second half (Q_{x2} , Q_{y2})). In other words, we define a diffusion constant D:

$$D = \log_{10} \sqrt{(Q_{y2} - Q_{y1})^2 + (Q_{x2} - Q_{x1})^2} .$$

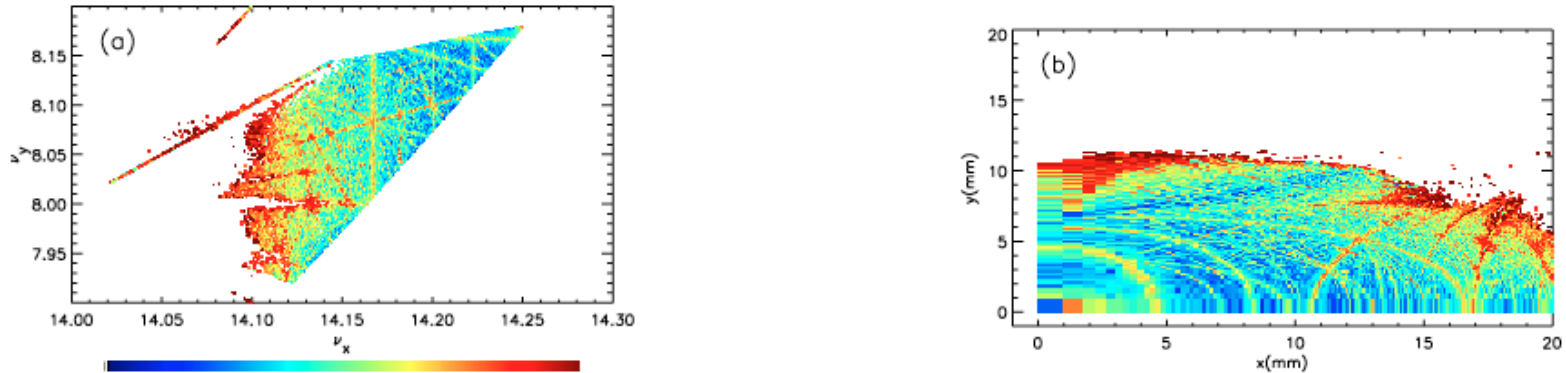


Fig. 13. The frequency map for an ideal lattice for ALS light source (LBNL) in tune space (a) and real space (b). The color scheme is logarithmic, with blue indicating completely stable motion and red/dark red indicating chaotic behavior close to complete loss of stability (white).

Nonlinear dynamics

Nonlinear effects in particle's motion in accelerators (or in Hamiltonian mechanics in general) some time can be treated in perturbative manner – the way we learned in this course. But while giving analytical expressions for the results, it is limited by – usually – second order perturbation and not necessarily converging when brought to higher orders. Needless to say it becoming very cumbersome even in the second order... Resonant approach, while giving a nice intuitive understanding of the resonances, is limited to (a) a single resonance, (b) ignores non-resonant terms which definitely distort or even – at large amplitude - ruin the simple picture we looked at. Fortunately there is a very systematic and rigorous method for non-linear dynamics developed by Prof. Alex J. Dragt (UM) and his follower (many of them his former students). This fundamental work started in late 1970s and brought to a well-formulated theory in early 1980s. Naturally, the work did not stopped there and there is a lot of new addition to this method (frequently oriented to computing and analyzing non-linear maps), which are extension of the method. Method itself is uses a number of mathematical concepts and power of Lie algebraic tools. It exploits symmetries of Hamiltonian systems and is – at present - the most comprehensive approach to the non-linear beam dynamics. We cannot follow each and every – some of them rather complex – derivations. Hence, we will deviate from tradition in our course to prove almost everything and will instead have a short introduction to this method. We may offer a dedicated course sometimes in near future.

Let's start from something we are well aware of: group (**G**) of $2n \times 2n$ symplectic matrices (formally called **Sp(2n)**) satisfying simplicity conditions:

$$\mathbf{M}^T \mathbf{S} \mathbf{M} = \mathbf{S}; \quad (26-1)$$

which satisfy group properties **G** :

1. It contains identity matrix **I**: since obvious $\mathbf{I}^T \mathbf{S} \mathbf{I} = \mathbf{S}$

2. If $\mathbf{M} \in \mathbf{G} \rightarrow \mathbf{M}^{-1} \in \mathbf{G}$ (contains inverse matrix) :

$$\mathbf{M}^T \mathbf{S} \mathbf{M} = \mathbf{S}; \textcircled{R} \mathbf{M}^{-1} = -\mathbf{S} \mathbf{M}^T \mathbf{S}; \textcircled{R} \mathbf{M}^T \mathbf{S} \mathbf{M} = \mathbf{S};$$

$$\mathbf{M}^{-1T} \mathbf{S} \mathbf{M}^{-1} = -\mathbf{S} \mathbf{M} \mathbf{S} \mathbf{M}^T \mathbf{S} = \mathbf{S}.$$

3. $\mathbf{M}, \mathbf{N} \in \mathbf{G} \rightarrow \mathbf{M} \cdot \mathbf{N} \in \mathbf{G}$: since $(\mathbf{M} \mathbf{N})^T \mathbf{S} \cdot \mathbf{M} \mathbf{N} = \mathbf{N}^T (\mathbf{M}^T \mathbf{S} \mathbf{M}) \mathbf{N} = \mathbf{N}^T \mathbf{S} \mathbf{N} = \mathbf{S}$

4. $\mathbf{M}(\mathbf{N} \mathbf{L}) = (\mathbf{M} \mathbf{N}) \mathbf{L}$, which is correct for any square matrices of the same order.

Thus, we proved that that symplectic matrices form symplectic group. Now we will focus on more formal definition of something we are familiar with, which is called lie algebraic properties. For any matrix **A** we defined exponential matrix function (heavily use in Lie algebras):

$$\exp(\mathbf{A}) = \sum_{n=0}^{\infty} \frac{\mathbf{A}^n}{n!}; \quad (26-2)$$

which converge for any **A** . A bit trickier is inverse, i.e. natural logarithm function:

$$\ln(\mathbf{A}) = \ln(\mathbf{I} - (\mathbf{I} - \mathbf{A})) = -\sum_{n=1}^{\infty} \frac{(\mathbf{I} - \mathbf{A})^n}{n}.; \quad (26-3)$$

uniqueness and convergence of which is much less trivial. It definitely converges when norm of $\mathbf{I} - \mathbf{A}$ is close to zero.

We know that for (real) matrix \mathbf{A} with non-zero eigen values (e.g. non-zero determinant!) we can use Sylvester formula and find (a bit trickier to get it to be real) a solution of (26-3). We are all aware that \ln of any number has branching at zero and is defined with accuracy of $2n\pi$. It means that $\mathbf{A} = \exp(\mathbf{B})$ has infinite number of solutions.

It is possible to show (a good exercise similar to proving $\exp(\ln(x))=x$) that if:

$$\mathbf{B} = \ln(\mathbf{A}) \rightarrow \mathbf{A} = \exp(\mathbf{B}). \quad (26-4)$$

If \mathbf{M} is real and symplectic, than

$$\mathbf{D} = \ln(\mathbf{M}) \rightarrow \mathbf{D}^T \mathbf{S} + \mathbf{S} \mathbf{D} = 0; . \quad (26-5)$$

or \mathbf{D} is anti-commute with \mathbf{S} . It is easy to prove:

$$\begin{aligned} \mathbf{D} = \ln(\mathbf{M}); -\mathbf{D} = \ln(\mathbf{M}^{-1}) &= \ln(\mathbf{S}^{-1} \mathbf{M}^T \mathbf{S}) = \mathbf{S}^{-1} \ln(\mathbf{M}^T) \mathbf{S} = -\mathbf{S} \ln(\mathbf{M}^T) \mathbf{S}; \\ \mathbf{D}^T = (\mathbf{S} \ln(\mathbf{M}^T) \mathbf{S})^T &= \mathbf{S} \ln(\mathbf{M}) \mathbf{S} = \mathbf{S} \mathbf{D} \mathbf{S}; \rightarrow \mathbf{D}^T - \mathbf{S} \mathbf{D} \mathbf{S} = -(\mathbf{D}^T \mathbf{S} + \mathbf{S} \mathbf{D}) \mathbf{S} = 0; \end{aligned} \quad (26-6)$$

It means that (surprise-surprise) that $\mathbf{D}=\mathbf{S}\mathbf{H}$, where \mathbf{H} is symmetric matrix:

$$\mathbf{H} = -\mathbf{S} \mathbf{D}; \mathbf{D}^T = \mathbf{S} \mathbf{D} \mathbf{S} \rightarrow \mathbf{H}^T = \mathbf{D}^T \mathbf{S} = \mathbf{S} \mathbf{D} \mathbf{S}^2 = -\mathbf{S} \mathbf{D} = \mathbf{H}. \quad (26-7)$$

We already proved many times that for $\mathbf{H}^T=\mathbf{H}$,

$$\mathbf{M} = \exp(\mathbf{S}\mathbf{H}) \rightarrow \mathbf{M}^T \mathbf{S} \mathbf{M} = \mathbf{S}, \quad (26-8)$$

which is a two-liner:

$$\begin{aligned} \mathbf{M}^T &= \exp((\mathbf{S}\mathbf{H})^T) = \exp(-\mathbf{H}\mathbf{S}) = \exp(-\mathbf{S}^{-1} \mathbf{S} \mathbf{H} \mathbf{S}) = \mathbf{S}^{-1} \exp(-\mathbf{S}\mathbf{H}) \mathbf{S} = \mathbf{S} \exp(-\mathbf{S}\mathbf{H}) \mathbf{S} \\ \mathbf{S}^{-1} &= -\mathbf{S}; \mathbf{M}^T \mathbf{S} \mathbf{M} = -\mathbf{S} \exp(-\mathbf{S}\mathbf{H}) \mathbf{S}^2 \exp(\mathbf{S}\mathbf{H}) = \mathbf{S} \exp(\mathbf{S}\mathbf{H} - \mathbf{S}\mathbf{H}) = \mathbf{S}. \end{aligned}$$

What we shown is that symplectic matrix can be written on form

$$\mathbf{M}^T \mathbf{S} \mathbf{M} = \mathbf{S} \rightarrow \mathbf{M} = \exp(\mathbf{S} \mathbf{H}), \mathbf{H}^T = \mathbf{H}. \quad (26-9)$$

Now we are ready to define Lie algebra for matrices: A set of matrices forms **Lie algebra** if:

1. If matrix **A** is in the Lie algebra, than so any product with a scalar **a**, **aA** ;
2. If matrices **A** and **B** is in the Lie algebra, then so their sum **A+B**.
3. If matrices **A** and **B** is in the Lie algebra, then so their commutator **[A,B]**, defined as

$$[\mathbf{A}, \mathbf{B}] = \mathbf{AB} - \mathbf{BA}, \quad (26-10)$$

which is something new we did not touched yet in our course, but something having a very fundamental relation with Poisson brackets in Hamiltonian mechanics. The next is to show that our **D=SH**, **H^T=H** set of matrices **D** form an Lie algebra. From observing that **H=-SD**, two first conditions are trivial adding symmetric matrices and multiplying them by a scalar keeps them symmetric. Third condition is a new and can be easily proved:

$$\mathbf{A} = \mathbf{S} \mathbf{H}_1, \mathbf{B} = \mathbf{S} \mathbf{H}_2; [\mathbf{A}, \mathbf{B}] = \mathbf{S} \mathbf{H}$$

$$\mathbf{H} = -\mathbf{S} [\mathbf{A}, \mathbf{B}] = \mathbf{S} \mathbf{B} \mathbf{A} - \mathbf{S} \mathbf{A} \mathbf{B} = \mathbf{H}_1 \mathbf{S} \mathbf{H}_2 - \mathbf{H}_2 \mathbf{S} \mathbf{H}_1; \quad (26-11)$$

$$\mathbf{H}^T = (\mathbf{H}_1 \mathbf{S} \mathbf{H}_2 - \mathbf{H}_2 \mathbf{S} \mathbf{H}_1) = (\mathbf{H}_2^T \mathbf{S}^T \mathbf{H}_1^T - \mathbf{H}_1^T \mathbf{S}^T \mathbf{H}_2^T) = \mathbf{H}_1 \mathbf{S} \mathbf{H}_2 - \mathbf{H}_2 \mathbf{S} \mathbf{H}_1 = \mathbf{H};$$

which proves that **[A,B]=SH** with **H^T = H**.

Further, is possible to prove that symplectic matrix can be presented in form of the product of exponents

$$\mathbf{M} = \exp(\mathbf{SH}_a) \exp(\mathbf{SH}_s), \mathbf{SH}_a = -\mathbf{H}_a \mathbf{S}; \mathbf{SH}_c = \mathbf{H}_c \mathbf{S}; \quad (26-12)$$

with commuting and anti-commuting generating matrices $\mathbf{H}_a, \mathbf{H}_c$. This can be proven using the fact that an arbitrary real non-singular matrix can be decomposed as product of real positive definite symmetric matrix \mathbf{P} and orthogonal matrix \mathbf{O} (we use it without prove!):

$$\mathbf{M} = \mathbf{PO}; \mathbf{P}^T = \mathbf{P}; \mathbf{O}^T = \mathbf{O}^{-1}; \quad (26-13)$$

For symplectic matrix we have

$$\mathbf{M} = \mathbf{S}^{-1} (\mathbf{M}^{-1})^T \mathbf{S} \rightarrow \mathbf{PO} = (\mathbf{S}^{-1} \mathbf{P}^{-1} \mathbf{S}) (\mathbf{S}^{-1} \mathbf{O} \mathbf{S})$$

where we used $\mathbf{P}^T = \mathbf{P}; \mathbf{O}^T = \mathbf{O}^{-1}$ and with $\mathbf{S}^{-1} \mathbf{P}^{-1} \mathbf{S}$ being real, symmetric and positive definite and $\mathbf{S}^{-1} \mathbf{O}^{-1} \mathbf{S}$ real and orthogonal. Since polar decomposition is unique (we use it without prove!) than

$$\mathbf{P} = \mathbf{S}^{-1} \mathbf{P}^{-1} \mathbf{S}; \mathbf{O} = \mathbf{S}^{-1} \mathbf{O} \mathbf{S}; \rightarrow \mathbf{P} = -\mathbf{S} (\mathbf{P}^{-1})^T \mathbf{S}; \mathbf{O} = -\mathbf{S} (\mathbf{O}^{-1})^T \mathbf{S};$$

$$\mathbf{P}^T \mathbf{S} \mathbf{P} = \mathbf{P}^T (\mathbf{P}^{-1})^T \mathbf{S} = \mathbf{S}; \quad \mathbf{O}^T \mathbf{S} \mathbf{O} = \mathbf{O}^T (\mathbf{O}^{-1})^T \mathbf{S} = \mathbf{S} \#$$

e.g. both of these matrices are symplectic. A bit more of exercises are needed to prove that $\mathbf{A} = \ln \mathbf{O}$ is asymmetric matrix $\mathbf{A}^T = -\mathbf{A}$ and $\mathbf{B} = \ln \mathbf{P}$ is symmetric matrix $\mathbf{B}^T = \mathbf{B}$:

$-\mathbf{A} = \ln \mathbf{O}^{-1} = \ln \mathbf{O}^T = \mathbf{A}^T; \mathbf{B}^T = \ln \mathbf{P}^T = \ln \mathbf{P} = \mathbf{B}$. As we found that for any logarithm of symplectic matrix condition (26-5) applies $\mathbf{D} = \ln(\mathbf{M}) \rightarrow \mathbf{D}^T \mathbf{S} + \mathbf{S} \mathbf{D} = 0$; requiring:

$$\begin{aligned} \mathbf{A}^T \mathbf{S} + \mathbf{S} \mathbf{A} &= 0 \rightarrow \mathbf{A} \mathbf{S} = \mathbf{S} \mathbf{A}; \mathbf{A} = \mathbf{S} \mathbf{H}_c \rightarrow \mathbf{H}_c \mathbf{S} = \mathbf{S} \mathbf{H}_c \\ \mathbf{B}^T \mathbf{S} + \mathbf{S} \mathbf{B} &= 0 \rightarrow \mathbf{B} \mathbf{S} = -\mathbf{S} \mathbf{B}; \mathbf{B} = \mathbf{S} \mathbf{H}_a \rightarrow \mathbf{H}_a \mathbf{S} = -\mathbf{S} \mathbf{H}_a \# \end{aligned} \quad (26-14)$$

This proves (relying on a couple of theorem from linear algebra we took for granted) that (26-12) is correct. Since, $\mathbf{S}^2 = -\mathbf{I} = (i\mathbf{I})^2$ and generating matrices either commute or anti-commute with \mathbf{S} , one can find real $\mathbf{H}_a, \mathbf{H}_c \dots$ again without proof.

Now we are ready to connect our – so far an abstract exercise – to Poisson brackets, which are defined for two functions of coordinates and momenta as

$$\begin{aligned}
 X &= \{x_i, i = 1, 2n\} = \{\{q_k, P^k\} k = 1, n\}; \\
 f &= f(X, s) \equiv f(q_k, P^k, s); g = g(X, s) \equiv g(q_k, P^k, s); \\
 [f, g]_{def} &= \sum_{k=1}^n \left(\frac{\partial f}{\partial q_k} \frac{\partial g}{\partial P^k} - \frac{\partial g}{\partial q_k} \frac{\partial f}{\partial P^k} \right) = \sum_{i,j=1}^{2n} \left(\frac{\partial f}{\partial x_i} S_{ij} \frac{\partial g}{\partial x_j} \right) = \\
 &(\partial_x f, \mathbf{S} \cdot \partial_x g) = (\partial_x f)^T \mathbf{S} \cdot (\partial_x g).
 \end{aligned} \tag{26-15}$$

From Hamiltonian mechanics we know that

$$\frac{df}{dt} = \frac{\partial f}{\partial t} + [f, H] = \frac{\partial f}{\partial t} + \frac{\partial f}{\partial X} S \frac{\partial H}{\partial X} = \frac{\partial f}{\partial t} + \frac{\partial f}{\partial q_k} \frac{\partial H}{\partial P^k} - \frac{\partial f}{\partial P^k} \frac{\partial H}{\partial q_k};$$

and time-independent function “commuting” with Hamiltonian are invariants of motion.